Advances in Materials Science and Engineering

Research Transcripts in Materials

Kishor B. Kale
Balasaheb S. Gandhare
Sham S. Kulkarni
Editors

1 Evaluation of Indium Tin Oxide Based Surface Plasmon Resonance Sensor for Near-IR Applications

Anjitha M[a], Niveditha Nair[a], Varsha T. Babu[a], Nishi G.N[b], Athulya S[a], Sharika E[a], Tauseef Ahmed[c,d], Mukul Kumar Das[c,d], Rita Rizzoli[e], Caterina Summonte[e] and Sanjay K. Ram[a,*]

[a]Department of Physics, Amrita Vishwa Vidyapeetham, Amritapuri, India
[b]Department of Electronics and Communication Engineering, Amrita Vishwa Vidyapeetham, Amritapuri, India
[c]Department of Electronics Engineering, IIT(ISM) Dhanbad, India
[d]Centre of Excellence in Renewable Energy, IIT(ISM) Dhanbad, India
[e]IMM-Consiglio Nationale delle Ricerche, via Gobetti 101, Bologna, Italy

*Corresponding author: sanjayk.ram@gmail.com

ABSTRACT

Surface plasmon resonance (SPR) based optical biosensors hold strong potential for high-speed detection of changes in optical properties resulting from the alteration of the chemical or biochemical composition of the analyte. Traditionally, noble metals have been investigated for such plasmonic properties, while alternative materials like metal oxides have recently attracted attention for the potential to be tuned for applications in different spectral regions. This chapter addresses the design of a highly sensitive biosensor based on a conducting oxide, indium tin oxide (ITO), for sensing in the near infra-red (NIR) range, up to wavelengths as low as the ones used in telecommunications (~1.55 μm). The analysis of the sensor performance leads us to introduce a new performance parameter, the comprehensive signal quality factor of the SPR curve, which is valuable to assess the quality of sensing. Our results also demonstrate the effectiveness of rf-magnetron sputtered ITO material, which has been less explored in literature for plasmonic applications.

Keywords: Surface plasmons, Kretschmann configuration, Transparent conducting oxides, Indium tin oxide, Biosensors, metal oxides

Advances in Materials Science and Engineering | ISBN: 978-81-948951-9-0
In Series: Research Transcripts in Materials | Vol: 01

1. INTRODUCTION

Biosensors used for monitoring the fluctuating surface optical properties in the sample environment pave the way to the detection of biological and chemical parameters, with many potential applications in pharmaceuticals, biotechnology, medical diagnostics, environmental analyses, and food probes. Optical biosensors hinged on surface plasmon resonance (SPR) offer a wide potential for the identification, detection, and quantification of biomolecules [1]. Traditional SPR sensors use noble metals like gold, silver, or Au-Ag films, which have the detrimental effect of high extinction losses as a result of interband transitions and free carrier absorption in the spectral regions of visible and near-infrared (NIR). Moreover, these noble metals are not compatible with CMOS technology and have limited tunability of their optical permittivities. This severely limits the practical implementation of the device on a Si-based platform. Over the last few years, low loss dielectric materials such as indium tin oxide (ITO), Al-doped ZnO (AZO), and gallium-doped ZnO (GZO) have turned up as a promising alternative in the form of low-loss plasmonic metamaterials for applications in the NIR regime [2 - 6].

ITO is a highly degenerate n-type semiconductor material having high free carrier density, low electrical resistivity, and a wide bandgap, allowing high transmission in the visible and NIR spectral range [7]. These attributes make ITO a popular material for applications in photovoltaics and opto-electronic devices [8]. The application of ITO for plasmonic and telecommunication in the NIR wavelength region ($\lambda \sim 1.55\ \mu m$) necessitates higher carrier concentration ($> 10^{21}\ cm^{-3}$) with good material quality [9]. Typically, the high quality, defect-free material required for such applications have been reported for the ITO deposited using PLD which is, however, not compatible with commercial production. Radio frequency magnetron sputtering (rf-MS) allows scalable fabrication of ITO with good optical and electrical properties, but the properties often fail to meet the superior criteria desirable for application in NIR plasmonics, limiting the research in this area.

In this work, we report on the study of rf-MS deposited ITO films for their plasmonic behavior in NIR region and evaluate their suitability for sensing applications. Our Kretschmann configuration based model manifests ITO as an exceptional substitute for noble metals for sensing in the NIR region.

2. EXPERIMENTAL DETAILS

Thin film layers of ITO were deposited on two types of substrates, <100> oriented c-Si and SCHOTT borosilicate glass using 13.6 MHz rf-MS system at a substrate temperature of 225 °C with Ar as sputtering gas [10]. Prior to the deposition of the ITO layers, the substrates were cleaned using routine RCA cleaning steps and then kept at 200 °C for some duration to remove moisture. The deposition parameters of ITO thin films growth at the rf-MS system are as follows: base pressure of ~ 2×10^{-7} Torr, gas pressure of 3 mTorr, rf-power of 50 W, Ar flow of 14.85 sccm.

The optical reflection and transmission (R&T) of the deposited films were measured using a double-beam spectrometer in a broad spectral range from 200 to 2000 nm. The electrical resistivity (ρ) of the samples was measured by the four-point probe method. To determine Carrier concentration (n) and carrier mobility (μ) of the films were determined from Hall effect measurement in the Van der Pauw configuration using a 1.2 T electromagnet. Spectroscopy ellipsometry was employed to measure the film thicknesses.

3. THEORETICAL BACKGROUND

A prism coupling method useful to generate surface plasmon resonance is the Kretschmann configuration where the incident beam of TM-polarized light passes along the interface of two dielectric materials with both positive and negative permittivity. This set-up is realized using a mechanical system and a prism to make the incident light fall obliquely on the metal/dielectric interface, and the SPR is generated at the interface. Fig. 1 demonstrates a schematic illustration of such a system.

For this excitation of surface plasmons to happen, the wavevector of the incident electromagnetic wave source (k_{beam}) should match the intrinsic wavevector of the surface plasmon polaritons (SPP) in the thin metallic layer ($k_{plasmon}$). Whenever the wavevectors of both the source and media matches, the phonon-photon coupling can generate a response, which is the surface plasmon resonance [11]. The wavevector of metal and sample are [11]:

$$k_{plasmon} = \frac{2\pi}{\lambda}\sqrt{\frac{\varepsilon_{metal} \times \varepsilon_{sample}}{\varepsilon_{metal} + \varepsilon_{sample}}} \qquad (1)$$

ε_{metal} and ε_{sample} in the equation are the complex dielectric permittivities of the metal and the dielectric medium (e.g. sample), respectively, which are the function of wavelength [11].

The incident wave vector can be expressed as:

$$k_{beam} = \frac{2\pi}{\lambda}\sqrt{n_{prism}\sin\theta} \qquad (2)$$

where $2\pi/\lambda$ is the wave vector of the incident angle, θ.

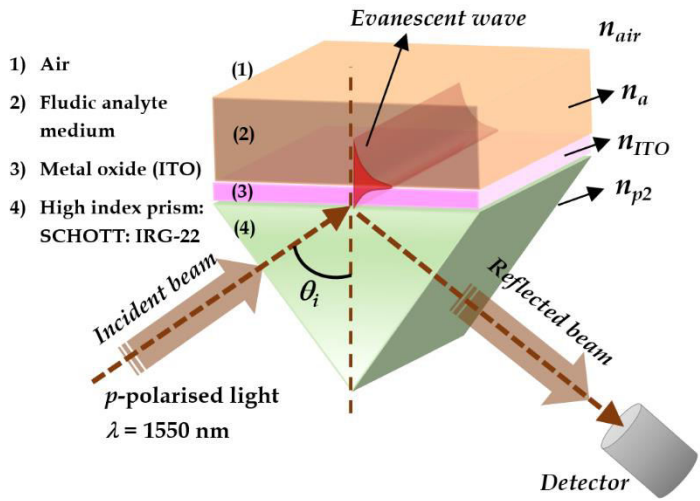

Fig. 1. Schematic illustration of the model setup of Kretschmann-Raether configuration for the excitation of SPR in attenuated total reflection situation. The components of the setup are mentioned in the picture

Matching the above two relationships of k_{beam} and $k_{plasmon}$ (i.e., $k_{beam} = k_{plasmon}$) gives the value of $\theta_{resonance}$ (minimum incident angle of the incoming electromagnetic wave) [11].

$$\theta_{resonance} = \sin^{-1}\left(\frac{\sqrt{\frac{\varepsilon_{metal} \times \varepsilon_{sample}}{\varepsilon_{metal} + \varepsilon_{sample}}}}{n_{prism}} \right) \tag{3}$$

From the above equation, we can conclude that the angle of incidence of the light, the characteristics of the coupling structure, and the test medium (through which the light traverses) can influence the relationship of wave vectors. The above dispersion equations are derived from an extensive treatment of Maxwell's equations with suitable applied boundary conditions.

The wave propagation in the frequency domain can be described by Maxwell's wave equation as:

$$\nabla \times \frac{1}{\mu_r}\left(\nabla \times E\right) - k_0{}^2 \left(\varepsilon_r - \frac{j\sigma}{\omega \varepsilon_0} \right) E \tag{4}$$

where, k_0 (wave vector of free space), ε_r (relative permittivity of material), E (electric field eqn.).

In this work, the required SPR response was implemented on COMSOL Multiphysics®, where the incident beam with 1550 nm propagates via a high indexed glass (SCHOTT IRG22) prism of 1.8 µm × 0.5 µm, an ITO layer of 1.8 µm × t and a dielectric layer of 1.8 µm × 0.5 µm. Schott IRG22 is a high index glass of the composition of $Ge_{33}As_{12}Se_{55}$ with a refractive index of 2.544 [12]. The incident beam is in TM mode with a wavelength of 1550nm and a power of 1W. The thickness of the ITO layer was varied from 90 nm to 160 nm. In COMSOL, the described structure has two ports. The Incident field is defined at the bottom active port and the top boundary where the reflected beam will be monitored is the passive port. The rest of the boundaries are defined as Floquet periodic boundaries, which can

secure the uniformity of the electric fields along and parallel to the interface [11]. After describing the required parameters, constraints, and material properties, the software automatically compiles the related equations described above internally using the Finite Element Method (FEM).

The optical parameters like the dielectric functions of the ITO layer used in the simulation model were obtained from the results of experimental reflection and transmission (R&T) measurements over a broad spectral region of films deposited on glass substrates. The experimental R&T spectral data were modeled using extended Drude and modified Lorentz oscillator model, the details of which can be found in an earlier report [13]. The deduced optical parameters were used to model the SPR behavior of this material.

4. RESULTS AND DISCUSSION

4.1. Optical properties of the ITO layer

The spectral dependence of the reflectance and transmittance of the rf-MS deposited ITO layer is shown in Fig. 2(a). The film achieves more than 85% of transmittance in the visible part of the spectrum. The drop in the transmittance values for the wavelengths, $\lambda > 1000$ nm with a simultaneous rise in the reflectance values can be attributed to the presence of free electron carriers. The optical parameters of this layer deduced from the optical modeling described in the above section is displayed in the Fig. 2(b) where the real part of the dielectric function, ε' corresponding to the left hand Y-axis and the imaginary part of the dielectric function, ε'' corresponding to the right hand Y-axis are plotted in the spectral range of 200 nm to 2000 nm. The crossover wavelength of this ITO film (i.e., when $\varepsilon' < 0$), shown in the Fig. 2(b) with an arrow indicates the value ~ 1160 nm, which is well below the telecommunication wavelength of 1550 nm. The expected spectral range of observing the SPPs at the interface of a conducting oxide and air is typically where the real part of the permittivity, ε' goes below –1. According to the data displayed in Fig. 2 (b), this wavelength is ~ 1300 nm for the ITO film in our study. The rise in the imaginary part of its permittivity, ε'' beyond this wavelength indicates optical losses and improvement in the metallic behavior of the film.

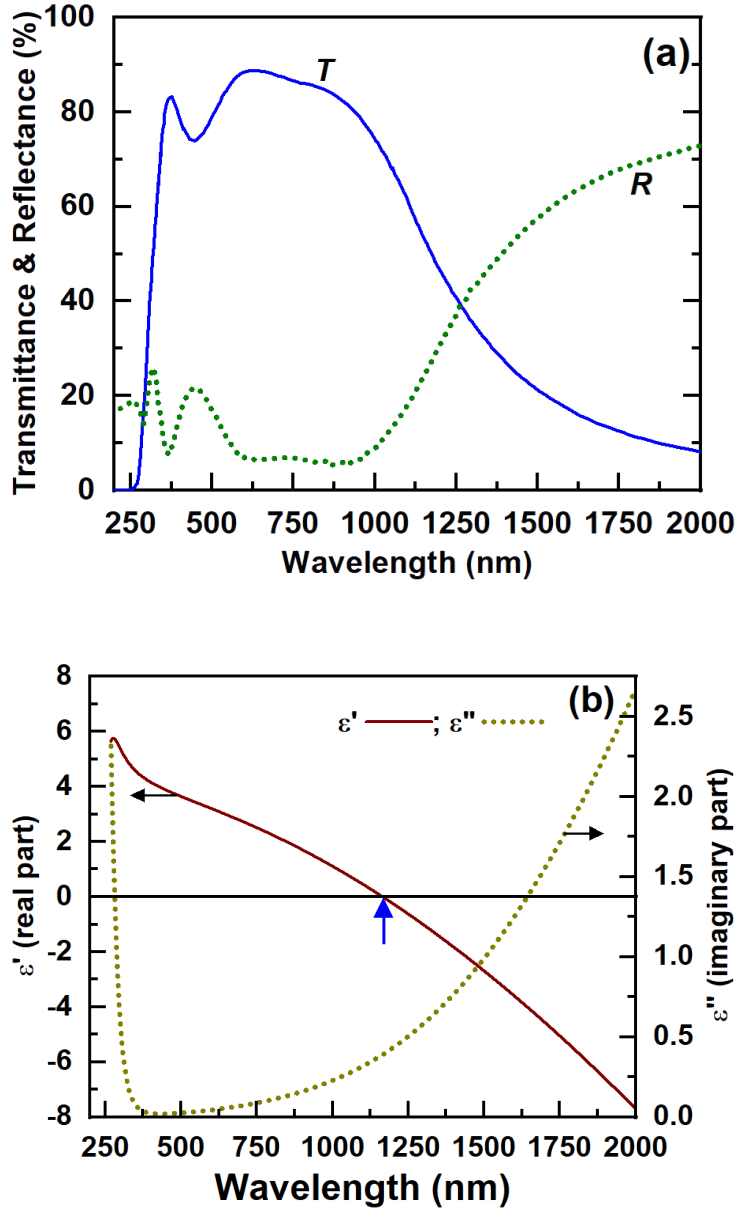

Fig. 2. (a) Transmission and reflection spectra of the ITO thin film deposited by rf-MS system. (b) the wavelength dependence of the optical parameters, real (ε') and imaginary part (ε'') of permittivity of the ITO film deduced from the optical modeling.

The electrical properties of this film obtained from Hall effect measurements are as follows: Hall resistivity, $\rho_{Hall} = 2.32\times10^{-4}$ (Ωcm); electron concentration, $n_{Hall} = 1.01\times10^{21}$ (cm^{-3}) and electron mobility, $\mu_{Hall} = 26.6$ (cm^2/Vs). The values of the electrical properties of the same film deduced from the optical modeling are as follows: optical resistivity, $\rho_{Opt} = 3.1\times10^{-4}$ (Ωcm); electron concentration, $n_{Opt} = 1.11\times10^{21}$ (cm^{-3}) and electron mobility, $\mu_{Opt} = 18.3$ (cm^2/Vs). The excellent corroboration of the experimentally obtained electrical properties with the theoretical optical models indicates the accuracy and reliability of the simulated models.

4.2. Thickness optimization of the ITO layer

The thickness of the metallic or conducting material layer is very crucial to observe SPR under the total internal reflection (TIR) condition of Kretschmann configuration apart from other geometrical constraints in the design of the structure. To study the dependence of SPR response on the material thicknesses and to identify an optimum thickness with the best SPR performance, the thicknesses of the $ITO_{rf\text{-}MS}$ layer were varied from 90 nm to 160 nm in the simulation model. Fig. 3 (a) represents the SPR curves of an ITO film where the dependence of reflectivity on the angle of incidence of light is shown.

4.3. SPR signal quality

The quality of the SPR signal can be deduced from many parameters: the full-width half-maxima (FWHM) of the curve (w) and the slope of the SPR curve (m), which signify the sharpness of the SPR curve (i.e., narrow FWHM and steep SPR curve); and larger reflectance difference (ΔR) and the lowest reflectance minima (R_{min}) at the SPR angle, which signify high signal-to-noise ratio, quality of the sensing data. Taking into account of all these parameters, a comprehensive signal quality factor of the SPR curve is introduced, $CQF_{SPR} = [log\ (R_{min})\times\Delta R\times m]/w$, having the unit as deg^{-2}. In Fig. 3 (b) quality of the SPR signal in terms of the SPR curve parameter, CQF_{SPR} is plotted against the corresponding thickness of the ITO layer. The optimum thickness for ITO is 130 nm with a θ_{SPR} of 28.4°, which corresponds to the highest CQF_{SPR} value [14]. The SPR signal quality in terms of ΔR

is ~ 0.76 for the rf-MS deposited ITO in this work, which is much higher compared to what is reported for the ITO material deposited using PLD technique [9].

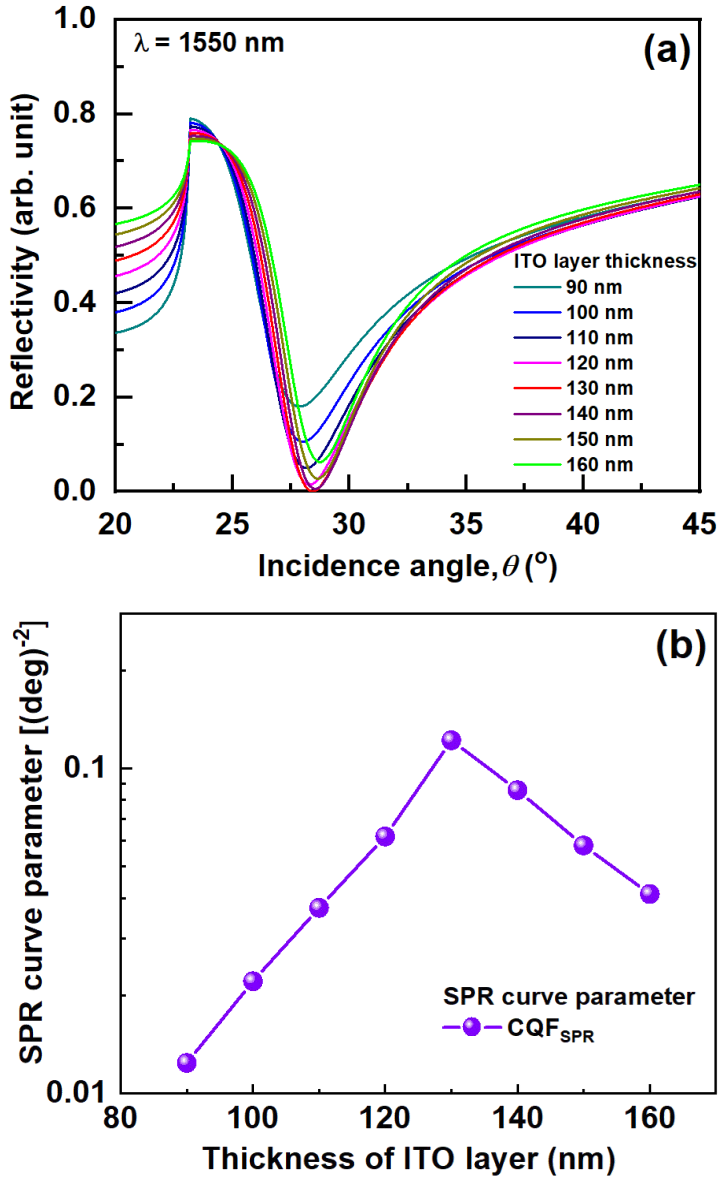

Fig. 3. (a) Angular dependence of SPR reflectivity of the ITO films of varying thicknesses. (b) Variation of SPR curve parameter, CQF_{SPR} w.r.t. the film thickness of the ITO films.

4.4. Sensing performance

For different analytes having different refractive indices, the resonance phenomenon is observed at different angles. The angular dip position θ_{SPR} also differs with the refractive indices of the prism materials, n_p. In this work, we tested the optical sensing performance of the sensor using ITO as a plasmonic material for the detection of the amount of hemoglobin (Hb) in the blood, since the refractive index of the blood changes with the varying amounts of hemoglobin (gram per liter) in it [15, 16].

The simulated SPR curves of the reflectivity vs angle of incidence of the ITO sensor having blood as an analyte is shown in Fig. 4 (a). The different SPR curves belong to the data of different blood samples having different Hb concentrations. The minima of the SPR curve shifts to the higher angles with the increase in the analyte's refractive index. The detection quality of the sensor is also judged by the displacement of the SPR angle, θ_{SPR} per unit change in the refractive index value (Δn). The Fig. 4 (b) shows a plot of SPR angle (θ_{SPR}) on the left Y-axis for the corresponding refractive index value of the analyte. The linear fit to the data gives the slope, indicating the sensing parameter, S (= $\Delta\theta_{SPR}/\Delta n$). The value of S for this ITO film at the wavelength of 1550 nm is 67.51 (°/RIU). The typical range of the values of the sensing parameter lies between 50 to 100 °/RIU for noble metals [14]. The right-hand side Y-axis of the Fig. 4 (b) shows the corresponding Hb amount in the blood with respect to the values of the refractive indices. The observation of SPR in a metal oxide film at the very low NIR wavelength (1550 nm) and the demonstration of its sensing capability has not been reported before. Our results indicate that with optimized fabrication, metal oxides can be cost-effective and practical alternatives to noble metals for plasmonic applications.

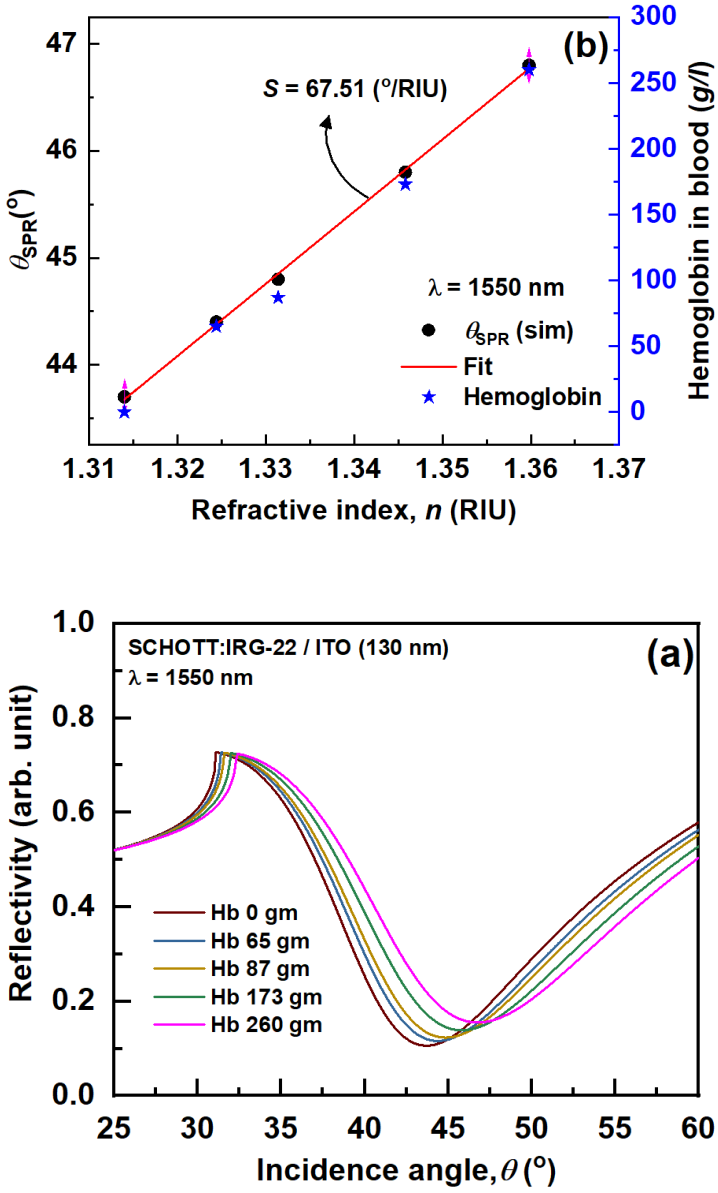

Fig. 4. (a) Angular dependence of SPR reflectivity of the ITO films on varying analyte conditions (Hemoglobin, Hb). (b) in the left Y-axis, shift in the SPR angle θ_{SPR} (°) on varying the refractive index of the analyte, Hb is shown while in the right Y-axis, the corresponding concentration of Hb in the blood is displayed.

5. SUMMARY AND CONCLUSION

The results of our experimental and theoretical studies substantiate the applicability of rf-MS deposited ITO material as a functionally suitable and industrially compatible plasmonic material for applications in the near-IR spectral range, especially in the telecommunications wavelength range. The analysis of the performance of the biosensor and the introduced performance parameter, the comprehensive signal quality factor of the SPR curve, are also useful for future optimization of sensing algorithms to realize highly sensitive sensors.

Acknowledgement

The Project has been carried out under a DST-SERB funded research project No. CRG/2019/006624.

Nomenclature

Ar	:	Argon
AZO	:	Al-doped zinc oxide
BK7	:	Borosilicate glass Schott
CMOS	:	Complementary metal oxide semiconductors
CQF	:	Comprehensive quality factor
FEM	:	Finite element method
FWHM	:	Full width half maximum
GZO	:	Gallium-doped zinc oxide
Hb	:	Hemoglobin
ITO	:	Indium tin oxide
NIR	:	Near infrared

PLD	:	Pulsed laser deposition
rf-MS	:	Radio frequency magnetron sputtering
RIU	:	Refractive index unit
SPP	:	Surface plasmon polariton
SPR	:	Surface plasmon resonance
TM	:	Transverse magnetic
S	:	Sensing parameter
ρ	:	Electrical resistivity
μ	:	Carrier mobility
n	:	Carrier concentration
θ	:	Incident angle
λ	:	wavelength
k_0	:	Wave vector of free space
m	:	Slope
w	:	FWHM
R	:	Reflectivity
n	:	Refractive index
ε	:	Relative permittivity
E	:	Electric field
σ	:	Electrical conductivity

REFERENCES

[1] A. Shalabney and I. Abdulhalim, Figure-of-merit enhancement of surface plasmon resonance sensors in the spectral interrogation, Optics Letters 37 (2012) 1175.

[2] A. Boltasseva and H. A. Atwater, Low-Loss Plasmonic Metamaterials, Science 331 (2011) 290.

[3] Y. Wang, A. Capretti and L. D. Negro, Wide tuning of the optical and structural properties of alternative plasmonic materials, Optical Materials Express, 5 (2015) 2415.

[4] A. Calzolari, A. Ruini, A. Catellani, Transparent Conductive Oxides as Near-IR Plasmonic Materials: The Case of Al-Doped ZnO Derivatives, ACS Photonics, 1 (2014) 703−709.

[5] P. R. West, S. Ishii, G. V. Naik, N. K. Emani, V. M. Shalaev, A. Boltasseva, Searching for better plasmonic materials, Laser & Photonics Reviews, 4 (2010) 795-808.

[6] P. K. Naini, J. Satapathy, E. M. Abhinav, A. Srinivas, M.M. Raja, Thermomagnetic Properties of Dy0.9Ho0.1MnO3 Multiferroics. physica status solidi (a), 217, 2000138 (2020).

[7] D. Desta, R. Rizzoli, C. Summonte, R. N. Pereira, A. N. Larsen, P. Balling and S. K. Ram, Nanomolded buried light-scattering (BLiS) back-reflectors using dielectric nanoparticles for light harvesting in thin-film silicon solar cells, EPJ Photovoltaics 11, 2 (2020).

[8] S. K. Ram, D. Desta, R. Rizzoli, B. P. Falcao, E. H. Eriksen, M. Bellettato, B.R. Jeppesen, P.B. Jensen, C. Summonte, R. N. Pereira, A. N. Larsen, P. Balling, Efficient light-trapping with quasi-periodic uniaxial nanowrinkles for thin-film silicon solar cells, Nano Energy 35, 341-349 (2017).

[9] J. Kim, G. V. Naik, N. K. Emani, A. Boltasseva, Plasmonic Resonances in Nanostructured Transparent Conducting Oxide Films, IEEE Journal of Selected Topics in Quantum Electronics, 19 4601907 (2013).

[10] I. G. Samatov, B. R. Jeppesen, A. N. Larsen, S. K. Ram, Room-temperature rf-magnetron sputter-deposited w-doped indium oxide: decoupling the influence of w dopant and o vacancies on the film properties, Applied Physics A 122, 458 (2016).

[11] T. Leelawattananon, K. Locharoenrat and S. Chittayasothorn, Simulation of Copper Thin Film Thickness Optimization for Surface Plasmon using the Finite Element Method, 7th International Conference on Simulation and Modeling Methodologies, Technologies and Applications (SIMULTECH 2017), pages 188-195.

[12] J. Le Persona, F. Colasa, C. Compèrea, M. Lehaitrea, M.-L. Anneb, C. Boussard-Plédelb, B. Bureaub, J.-L. Adamb, S. Deputierc and M. Guilloux-Viryc, Surface plasmon resonance in chalcogenide glass-based optical system. , Sensors and Actuators B: Chemical March 2008, Volume 130, Issue 2, Pages 771-776.

[13] C. Summonte, M. Allegrezza, M. Canino, M Bellettato and A. Desalvo, Analytical Expression for the Imaginary Part of the Dielectric Constant of Microcrystalline Silicon, RAM 2013, 1(1): 6-11.

[14] J. Vlčeka, J. Pištorab, M. Lesňák, Sensitivity enhancement in surface plasmon resonance sensors –theoretical modeling, Proc. of SPIE Vol. 7356 (2009) 735622.

[15] Ekaterina N. Lazareva, Valery V. Tuchin, Measurement of refractive index of hemoglobin in the visible/NIR spectral range, Journal of Biomedical Optics 23, 035004 (2018).

[16] J. Perayil, N. Suresh, A. Fenol, R. Vyloppillil, A. Bhaskar, S. Menon, Comparison of glycated hemoglobin levels in individuals without diabetes and with and without periodontitis before and after non-surgical periodontal therapy. Journal of periodontology, 85, 1658-1666 (2014)

Cite this article

Anjitha M, Niveditha Nair, Varsha T. Babu, Nishi G. N, Athulya S, Sharika E, Tauseef Ahmed, Mukul Kumar Das, Rita Rizzoli, Caterina Summonte and Sanjay K. Ram, "Evaluation of Indium Tin Oxide Based Surface Plasmon Resonance Sensor for Near-IR Applications," in *Advances in Materials Science and Engineering*, Kishor B. Kale, Balasaheb S. Gandhare, Sham S. Kulkarni, Ed. Pune, India: Grinrey Publishing, 2021, ch. 1, pp. 1-16.

Book Series by Grinrey Publishing

- Research Transcripts in Energy
- Research Transcripts in Engineering
- Research Transcripts in Materials
- Research Transcripts in Computer, Electrical and Electronics Engineering

www.grinrey.com

ISBN 978-81-948951-9-0